Synchrotron Small-Angle X-ray Scattering Studies on Phase Separation and Crystallization of Associated Polymer Blends

Katsuhiro Inomata,[†,‡] Li-Zhi Liu,[†] Takuhei Nose,[§] and Benjamin Chu*[,†]

Department of Chemistry, State University of New York at Stony Brook, Stony Brook, New York 11794-3400, and Department of Polymer Chemistry, Tokyo Institute of Technology, 2−12−1 Ookayama, Meguro-ku, Tokyo 152-8552, Japan

Received April 14, 1998; Revised Manuscript Received October 26, 1998

ABSTRACT: Time-resolved synchrotron small-angle X-ray scattering (SAXS) measurements during isothermal crystallization of an associated polymer blend, consisting of one-end-aminated polystyrene (APS) and one-end-sulfonated poly(ethylene glycol) (SPEG), have been performed. Two different methods of sample preparations were used. In the solvent cast method, the slowly evaporated APS/SPEG/toluene ternary solution should pass through the phase-separated region in the phase diagram. In the freeze−dry method, the solvent benzene was quickly frozen and then evaporated under vacuum, preventing the associated copolymer from dissociation. The freeze−dry sample exhibited similar microphase separation and crystallization behavior as that of the semicrystalline− (hard−) amorphous diblock copolymers with symmetric compositions. The interdomain distance of the freeze−dry sample remained relatively constant when SPEG was being crystallized. On the other hand, both microphase and macrophase separation occurred in the solvent-cast sample, resulting in an appreciably lowered scattered intensity when compared with that of the freeze−dry sample. In quenching from the melt state to 30 °C, the long period of the solvent-cast sample increased with time, similar to the behavior of the SPEG homopolymer when it was quenched from its melt state to 42 °C. However, this behavior is different from that of the freeze−dry sample which exhibited mainly crystallization behavior in the microphase domain. The difference in the formation of micro- and macrophases of the two samples in the melt state is responsible for the difference in the rate of crystallization of these samples, i.e., the rate of crystallization of homopolymer > that of solvent-cast blend sample > that of freeze−dry blend sample because the freeze−dry sample has the smallest region available for the crystallization of SPEG.

Introduction

Blend systems consisting of two polymers that are able to associate with each other by means of functional groups at one end of each polymer may exhibit a wide variety of phase behavior according to the strength of the association of the end groups and the segmental segregation strength.[1−8] When the association between the terminal groups is weak, the mixture may behave like an ordinary polymer blend, and macroscopic phase separation can occur. When the association strength is strong, the oppositely charged polymer pair will form a diblock copolymer (Figure 1). Studies of phase diagrams of associated polymer blend solutions in a good solvent have been reported recently.[1,2] For the system containing one-end-aminated polystyrene (APS), one-end-sulfonated poly(ethylene glycol) (SPEG) (Figure 1), and toluene, the strong association between the terminal amino group of APS and the terminal sulfonic acid group of SPEG promoted the miscibility of polystyrene (PS) and poly(ethylene glycol) (PEG), especially around the stoichiometric composition.[2] In the resulting phase diagram for APS/SPEG in toluene, the cloud-point curve had two peaks. The phase behavior for APS/SPEG/toluene could not be interpreted quantitatively by the Flory−Huggins type theory, and the existence of ordered microphase-separated structures became plausible.[2] Small-angle X-ray scattering (SAXS) studies of these

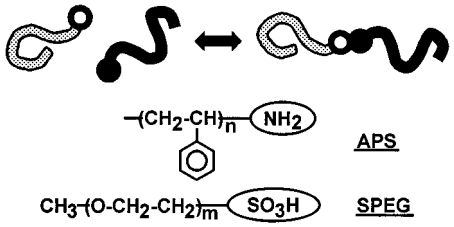

Figure 1. Schematics of the associated polymer blend by using two interacting terminal groups and chemical structure of APS and SPEG.

blends and blend solutions also suggested the formation of diblock-copolymer-like structures in the strongly associated APS/SPEG and APS/SPEG/toluene at 80 °C by the presence of a scattering maximum in the SAXS profile.[3]

In the strongly associated blends, the associated pair of APS and SPEG will form a semicrystalline−amorphous diblock copolymer. Crystallization of a crystalline−amorphous diblock copolymer is reported to lead to a richer variety of interesting morphologies.[9−29] In the melt state of a diblock copolymer, various ordered structures, such as lamellae, hexagonally packed cylinders and body-centered cubic spheres, are stable below the order−disorder transition (ODT), depending on the composition of the copolymer, the degree of polymerization, and the interaction parameter between the segments of each block.[30,31] Ordering by crystallization from the ordered melt is expected to compete with the existing microphase-separated structure and is influenced by the power of segregation of each segment (i.e. how far it is from the ODT) and by the state of the amorphous block (such as rubbery and glassy). Similar

* To whom correspondence should be addressed.
[†] State University of New York at Stony Brook.
[‡] Present address: Department of Polymer Chemistry, Tokyo Institute of Technology, 2-12-1 Ookayama, Meguro-ku, Tokyo 152-8552, Japan.
[§] Tokyo Institute of Technology.

10.1021/ma980576x CCC: $18.00
Published on Web 02/13/1999

Table 1. Characteristics of Sample Polymers

	code	M_w[a]	M_w/M_n[b]	F[c]
one-end-aminated polystyrene	APS	5.6×10^3	1.06	1.00
one-end-sulfonated poly-(ethylene glycol)	SPEG	5.7×10^3	1.05	0.99

[a] Determined by M_n and M_w/M_n, where M_n was measured by vapor-pressure osmometry. [b] Determined by size exclusion chromatography. [c] Functionalities of amino and sulfonic acid groups.

phase behavior can also be expected in the associated polymer blend with a strong association between the one-end functional groups. In this work, we performed time-resolved synchrotron SAXS measurements during an isothermal crystallization of SPEG, to investigate the morphology and crystallization behavior for the associated APS/SPEG polymer blend. Two different methods were adopted to prepare the blend samples. Depending on the method of sample preparation, we could observe two different kinds of growing processes of the SAXS peak during the crystallization of SPEG chains, due to the existence of two different phase separation structures before the crystallization process.

Experimental Section

Characteristics of the one-end-functional polymers used in this study, APS and SPEG, have been described in the previous reports[2,3] and are listed in Table 1. The two polymers have nearly identical molecular weights. The blend composition of APS/SPEG was set at 50/50 wt %. A blend sample, designated as APS/SPEG-SC, was prepared by evaporating the toluene (good solvent for both PS and PEG) solution under atmospheric pressure at room temperature, followed by drying in a vacuum, and annealed at 70 °C for 2 h. As suggested by the phase diagram in ref 2, APS/SPEG-SC should pass through a biphasic region during the solvent-evaporation process. The morphology formed during the solvent evaporation should remain because the annealing temperature was lower than T_g of APS (85 °C, determined by the differential scanning calorimetry (DSC) heating diagram). The other blend sample, APS/SPEG-FD, was prepared from a dilute benzene solution. After removing the solvent by the freeze−dry method, APS/SPEG-FD was annealed at 90 °C for 20 h in a vacuum. The long-time annealing at the temperature slightly higher than T_g is expected to enhance the order of the morphology formed during the freeze−dry process.

Synchrotron SAXS measurements were carried out at the SUNY X3A2 beamline and the Advanced Polymers Beamline at X27C, National Synchrotron Light Source (NSLS), Brookhaven National Laboratory (BNL).[32] A linear position-sensitive detector was used along with a pinhole collimation system and a temperature-jump sample cell. A wavelength (λ) of 0.128 nm for X3A2 and 0.131 nm for X27C was used. The lowest limit of $q = (4\pi/\lambda) \sin \theta$ (with 2θ being the scattering angle) was $\sim$0.1 nm^{-1}. The blend samples and pure SPEG were heated at a temperature above the melting point of SPEG (55 °C, determined by DSC heating diagram) and quickly moved into the measurement cell at a temperature below the crystallization temperature of SPEG. Measurements were started within 40 s after moving the sample to the measurement sample chamber. The temperature uncertainty of the sample just after the quench should not affect our studies because the crystallization process for all the samples took place over a long time period (more than 1200 s for the blends). The excess scattered intensity I_0 was obtained after attenuation, incident intensity fluctuation, and air scattering corrections.

Results and Discussions

The observed SAXS intensity, I_{obs}, was obtained after using a smoothing procedure (eq 1) of the corrected excess scattered intensity, I_0, to enhance the signal-to-noise ratio.

$$I_{obs}{}^{i} = (I_{obs}{}^{i-n} + I_{obs}{}^{i-n+1} + ... + I_{obs}{}^{i-1} + I_0{}^{i} + I_0{}^{i+1} + ... + I_0{}^{i+n-1} + I_0{}^{i+n})/(2n + 1) \quad (1)$$

($I_{obs}{}^1$, $I_{obs}{}^2$, ..., $I_{obs}{}^m$) and ($I_0{}^1$, $I_0{}^2$, ... $I_0{}^m$) are the linear array of smoothed and original scattering intensities, respectively. The invariant Q is defined as an integral of the SAXS intensity after Lorentz correction over q.[33]

$$Q = \int_0^\infty (I_{obs} - I_b) \exp(\sigma^2 q^2) q^2 \, dq \quad (2)$$

In this equation, I_b is the contribution from local electron density fluctuations in the amorphous phase (liquid scattering) of the Vonk type polynomial, and σ is related to the thickness of the crystalline-amorphous interphase. Before the calculation of Q, the SAXS data were extrapolated to both high and low q values. The extrapolation to high q was performed with the aid of the Porod law given in eqs 3 and 4. Once the Porod

$$\lim_{q \to \infty} [K - (I_{obs} - I_b) q^4 \exp(\sigma^2 q^2)] = 0 \quad (3)$$

$$\int_0^\infty [K - (I_{obs} - I_b) q^4 \exp(\sigma^2 q^2)] \, dq = 0 \quad (4)$$

constant K, the liquid scattering profile I_b, and the interface correlation term σ have been estimated, the invariant Q can be calculated by means of eq 2. The long period, D, was determined from the q value of the peak maximum in the Lorentz-corrected SAXS profile; i.e., $D = 2\pi/q$.

1. Phase Behavior Dependence on Sample Processing Procedures. In the present work, the APS/SPEG-SC and APS/SPEG-FD samples were quenched from the melt state ($\sim$75 °C) to 30 and 29 °C, respectively, to study the crystallization dynamics of the SPEG component. Their Lorentz-corrected time-resolved SAXS scattering curves are shown in parts a and b of Figure 2, respectively. It is seen from Figure 2 that just after the temperature jump from the melt state to the crystallization temperature (29−30 °C), both samples showed a residual peak in the SAXS profile (filled circles in Figure 2), which was not seen in Figure 3 for the pure SPEG homopolymer sample quenched from the melt state to 42 °C. We used the 42 °C temperature for the homopolymer crystallization because if the quench were from the melt state to 30 or 29 °C, the crystallization process would be too fast for us to follow. Our previous study[3] showed that a scattering maximum corresponding to microphase separation was observed in the melt state for this associated polymer system, suggesting the association between the terminal amino group of APS and the terminal sulfonic acid group of SPEG to form a diblock copolymer of the type as shown in Figure 1. Similarly, the residual scattering peaks in Figure 2 before crystallization could be attributed to the microphase separation structure of the samples. It is seen from Figure 2 that the SAXS peak for APS/SPEG-FD was more intense than that for APS/SPEG-SC. The annealing of the APS/SPEG-FD sample at 90 °C, slightly higher than the T_g of the APS component, could result in a better developed microphase structure than that of the solvent-cast sample. The higher scattered intensity of the freeze−dry sample when compared with that of the solvent-cast sample could be attributed to a

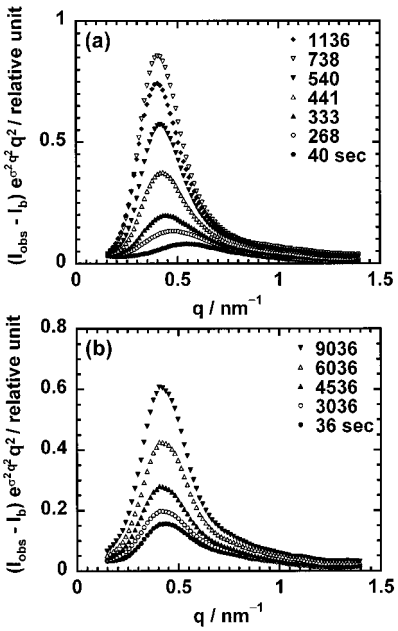

Figure 2. (a) Lorentz-corrected SAXS profiles of APS/SPEG-SC at different times as indicated after quenching from 70 to 30 °C. (b) Lorentz-corrected SAXS profiles of APS/SPEG-FD at different times as indicated after quenching from 80 to 29 °C.

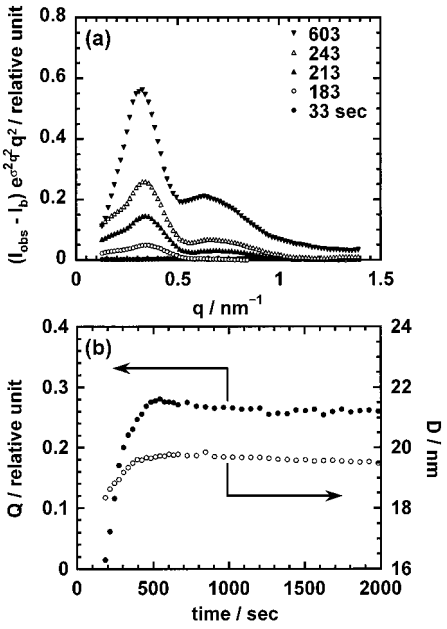

Figure 3. (a) Lorentz-corrected SAXS profiles of SPEG at different times as indicated after quenching from 80 to 42 °C. (b) Time dependence of invariant Q (filled circles) and long period D (open circles) obtained from the SAXS profiles of SPEG after quenching from 80 to 42 °C.

better developed microphase structure in the freeze−dry sample. On the other hand, the slowly evaporated APS/SPEG/toluene ternary solution should pass through the phase-separated region in the phase diagram during the preparation process of APS/SPEG-SC.[2] This means that the influence used to segregate APS and SPEG will overcome the association strength between the terminal amino and sulfonic acid groups. As the molecular weights of the unassociated homopolymers are the same as their corresponding blocks in the associated APS/SPEG block copolymer, the compatibilty of the formed diblock copolymer and the unassociated homopolymers

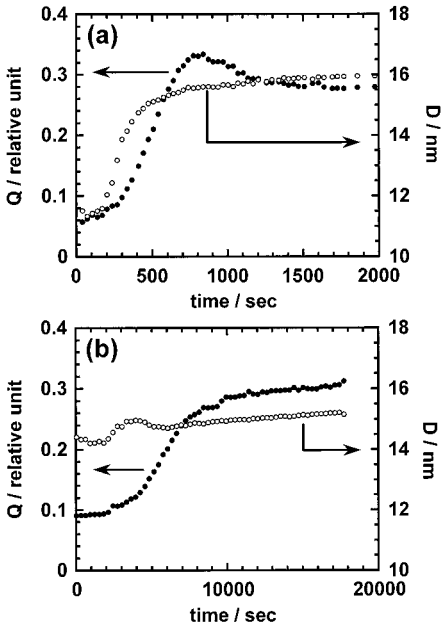

Figure 4. Time dependence of invariant Q (filled circles) and long period D (open circles) obtained from the SAXS profiles of (a) APS/SPEG-SC after quenching from 70 to 30 °C, and (b) APS/SPEG-FD after quenching from 80 to 29 °C.

should be relatively poor. Thus, a macrophase separation into APS-rich and SPEG-rich phases could occur during the solvent evaporation process. Unlike the solvent-cast sample, the freeze−dry sample, which did not pass through the macrophase-separated region during the sample preparation, should contain less unassociated homopolymers, which should be another reason the residual scattered intensity of the freeze−dry sample was considerably larger than that of the solvent-cast sample. The other difference in the two residual scattering maximum is that the freeze−dry sample showed a maximum at an appreciably lower q value than that of the solvent cast sample, indicating that the former had a considerably larger interdomain distance than the later.

It is noted that the residual scattering peaks in Figure 2, resulting from microphase separation, are appreciably broader than those normally seen for monodispersed block copolymers. The broadness of the SAXS peaks could correspond to the less organized microphase structures in our system as well as the presence of a certain amount of unassociated ASP and SPEG homopolymers. Further association of the end groups could have a negative effect on the formation of uniform microdomains. The broad SAXS peak for the freeze−dry sample, prepared with nearly monodispersed homopolymers and annealed for 20 h above the T_g of the ASP before measurement, suggests that it was difficult for the two end-functional homopolymers to totally associate into a pure diblock copolymer. The freeze−dry method was the more effective approach to form the associated copolymers. The dependence of phase behavior on different sample processing procedures can be further confirmed by the crystallization behavior discussed below.

2. Time-Resolved Study on Crystallization. Figure 2b shows that the Lorentz-corrected SAXS peak intensity of APS/SPEG-FD gradually increased with increasing time, without changing the peak position. The peak intensity of APS/SPEG-SC also increased with

increasing time (Figure 2a), although the change in the SAXS profile of APS/SPEG-SC was faster than that of APS/SPEG-FD. The position of the scattering peak of APS/SPEG-SC shifted to the smaller-angle region at the beginning of the crystallization process, i.e., the peak located at ca. 0.47 nm^{-1} up to the elapsed time of 137 s and at ca. 0.36 nm^{-1} after the elapsed time period of 268 s. This kind of change in the SAXS profile was not observed after an elapsed time of ca. 300 s. Figure 2a also indicates that the peak intensity of the APS/SPEG-SC decreased with time after $t \cong 800$ s (see the profiles at 738 and 1136 s). However, the Lorentz-corrected SAXS profiles of APS/SPEG-FD in Figures 2b showed that the SAXS peak was located at almost the same position during the crystallization of SPEG, and that the peak intensity increased monotonically with the elapsed time after the quenching. The invariant Q and the long period D, obtained from the Lorentz-corrected SAXS profile, are plotted as a function of the elapsed time after quenching in Figure 4. For APS/SPEG-SC (Figure 4a), D approached a constant value gradually after an initial rapid increase, while for the freeze−dry sample, D remained at a nearly constant value (∼15 nm) with time. The Lorentz-corrected SAXS profiles of pure SPEG during the isothermal crystallization at 42 °C (Figure 3a) shows that with increasing time, higher-order peaks at the higher q region could be observed in addition to the main peak. The obtained invariant Q and the long period D are plotted against the elapsed time after quenching in Figure 3b. The long period showed a slight increase with time, implying a thickening of the lamellar layers during the isothermal crystallization.[34,35]

From the above results and the crystallization condition (temperature) adopted for each sample, it can be seen that the crystallizability of the associated polymer system was also different when the sample processing procedures were different. As the APS/SPEG-FD sample was quenched to a lower temperature (29 °C), instead of 30 °C for the APS/SPEG-SC sample, one could expect that the crystallization of the former was faster than the later, if only the temperature effect was considered. However, Figure 4 shows that the invariant value Q levels off at about 20 min for the solvent-cast sample, while it levels off at about 3 h for the freeze−dry sample, indicating that the crystallization in the freeze−dry sample is much slower than that in the solvent-cast sample. The much faster crystallization rate of the solvent-cast sample also suggests that more unassociated SPEG homopolymers were present in this sample. When a symmetric APS/SPEG diblock copolymer was formed by association, it was supposed to form an alternating APS and SPEG lamellar structure. The interlamellar distance should be relatively constant regardless of SPEG crystallization. This is because the microphase separation structure has been frozen below the T_g of the APS component (about 85 °C). A similar phenomenon has also been reported for the poly(tetrahydrofuran-*b*-methyl methacrylate) diblock copolymer system with hard PMMA microdomains.[29] The almost constant interdomain distance in Figure 2b suggested that there was no SPEG-rich macrophase formed in the freeze−dry sample; i.e., a nearly pure microphase separation in this sample was suggested. The crystallization of SPEG chains in the freeze−dry sample took place in the confined SPEG microphase domains, while crystallization of the solvent-cast sample partially occurred in the SPEG-rich macrophase. The size dimension and the conformational constraints in the freeze−dry sample limited its crystallizability and resulted in a slower crystallization rate than that of the solvent-cast sample.

The solvent-cast sample showed a similar change in the long period with time (Figure 4a) as that of the SPEG homopolymer (Figure 3); i.e., its long period increased with time by more than 30% in the early stage of the crystallization process (Figure 4a). The similarity of the associated sample to the pure homopolymer could be related to the SPEG-rich macrophase in the solvent-cast associated sample. The time-resolved experiment showed that the crystallization rate of the solvent-cast associated sample was much slower than that of the SPEG homopolymer. For our experiment, the SPEG homopolymer was crystallized at 42 °C (the crystallization temperatures of 29 and 30 °C, which were adopted for the blend samples, were too low to observe the dynamics of crystallization behavior for pure SPEG). The much slower crystallization rate of the solvent-cast associated sample than that of the SPEG homopolymer suggested that the association of the APS and SPEG in the solvent-cast sample had substantially slowed the crystallization of the SPEG component.

In APS/SPEG-SC, the Q value has a maximum before reaching a constant value, while the Q value for APS/SPEG-FD increases monotonically to a constant value. An increase in Q during the crystallization process is due to an increase in the electron density difference between APS-rich and SPEG-rich microdomains by the crystallization of SPEG because the electron density increases in the order of amorphous PS ($\rho_{APS} = 346$ e/nm^3), amorphous PEG ($\rho_{am} = 369$ e/nm^3), and crystalline PEG ($\rho_{cr} = 403$ e/nm^3). The invariant for the three-component system consisting of APS, crystalline SPEG (cr), and amorphous SPEG (am) is defined as[36]

$$Q = (\bar{\rho} - \rho_{APS})^2\phi_{APS} + (\bar{\rho} - \rho_{cr})^2\phi_{cr} + (\bar{\rho} - \rho_{am})^2\phi_{am} \quad (5)$$

$$\bar{\rho} = \rho_{APS}\phi_{APS} + \rho_{cr}\phi_{cr} + \rho_{am}\phi_{am} \quad (6)$$

where ρ and ϕ represents the electron density and volume fraction of each component. Numerical calculation suggests that eq 5 can explain the existence of the maximum in Q plotted against the crystallization time. For a semicrystalline homopolymer, eqs 5 and 6 can be simplified as follows.

$$Q = \phi_{cr}\phi_{am}(\rho_{cr} - \rho_{am})^2 = \phi_{cr}(1 - \phi_{cr})(\rho_{cr} - \rho_{am})^2 \quad (7)$$

Equation 7 suggests that Q has a maximum at $\phi_{cr} = 0.5$ with a constant electron density contrast[12] and can explain the small maximum at $t = 500$ s in the plot of Q against the elapsed time for the crystallization of pure SPEG (Figure 4b). A similar phenomenon should occur in APS/SPEG-SC, i.e., crystallization of SPEG in the SPEG-rich macrophase will increase ϕ_{cr} and decrease ϕ_{am} under the constant value of ϕ_{APS} in eq 5. It should be noted that the correlation between APS-rich and SPEG-rich macrophases is not included in the experimentally obtained value of Q, because the corresponding q value should be smaller than the lower limit of observed q. The contribution from the crystallization of SPEG in the APS-rich macrophase can be ignored

because of the high glass transition temperature of the APS-rich phase.[37]

Conclusions

Our time-resolved SAXS studies show that processing procedures of the associated system, consisting of one-end-aminated polystyrene and one-end-sulfonated poly(ethylene glycol), can greatly influence its micro- and macrostructures and hence influence the crystallization process. The freeze−dry method could be used to prepare an APS/SPEG associated sample. The resulting sample has much less unassociated APS and SPEG homopolymers than those in the solvent-cast sample. The crystallization behavior of the freeze−dry sample is similar to that of a semicrystalline− (hard−) amorphous diblock copolymer with a symmetric composition. The crystallization behavior of the solvent-cast sample is similar to that of the pure SPEG homopolymer, due mainly to the presence of SPEG-rich macroscopic regions.

Acknowledgment. The authors thank Professor S. Nakahama of the Tokyo Institute of Technology for kindly providing the functional polymers in this study. B.C. gratefully acknowledges support of this work by the Department of Energy (DEFG0286ER45237·014), the National Science Foundation (DMR9612386 and DMR9632525), and the U.S. Army Research Office (DAAG559710022), as well as the Advanced Polymers Beamline at X27C and the SUNY Beamline at X3A2 at NSLS, BNL.

References and Notes

(1) Haraguchi, M.; Nakagawa, T.; Nose, T. *Polymer* **1995**, *36*, 2567.
(2) Haraguchi, M.; Inomata, K.; Nose, T. *Polymer* **1996**, *37*, 3611.
(3) Inomata, K.; Haraguchi, M.; Nose, T. *Polymer* **1996**, *37*, 4223.
(4) Russell, T. P.; Jerome, R.; Charlier, P.; Foucart, M. *Macromolecules* **1988**, *21*, 1709.
(5) Iwasaki, K.; Hirao, A.; Nakahama, S. *Macromolecules* **1993**, *26*, 2626.
(6) Iwasaki, K.; Tokiwa, T.; Hirao, A.; Nakahama, S. *Polym. Prepr. Jpn.* **1992**, *41*, 1893; Iwasaki, K.; Hirao, A.; Nakahama, S. *Polym. Prepr. Jpn.* **1993**, *42*, 1419.
(7) Tanaka, F. *Macromolecules* **1989**, *22*, 1988; *Macromolecules* **1990**, *23*, 3784, 3790.
(8) Tanaka, F.; Ishida, M.; Matsuyama, A. *Macromolecules* **1991**, *24*, 5582.
(9) Gervais, M.; Gallot, B. *Makromol. Chem.* **1973**, *171*, 157; *Makromol. Chem.* **1973**, *174*, 193.
(10) Gallot, B. R. M. *Adv. Polym. Sci.* **1978**, *29*, 85.
(11) Hirata, E.; Ijitsu, T.; Soen, T.; Hashimoto, T.; Kawai, H. *Polymer* **1975**, *16*, 249.
(12) Yang, Y-.W.; Tanodekaew, S.; Mai, S.-M.; Booth, C.; Ryan, A. J.; Bras, W.; Viras, K. *Macromolecules* **1995**, *28*, 6029.
(13) Mai, S.-M.; Fairclough, J. P. A.; Hamley, I. W.; Matsen, M. W.; Denny, R. C.; Liao, B.-X.; Booth, C.; Ryan, R. J. *Macromolecules* **1996**, *29*, 6212.
(14) Ryan, A. J.; Fairclough, J. P. A.; Hamley, I. W.; Mai, S.-M.; Booth, C. *Macromolecules* **1997**, *30*, 1723.
(15) Khandpur, A. K.; Macosko, C. W.; Bates, F. S. *J. Polym. Sci., Polym. Phys. Ed.* **1995**, *33*, 247.
(16) Ryan, A. J.; Hamley, I. W.; Bras, W.; Bates, F. S. *Macromolecules* **1995**, *28*, 3860.
(17) Hamley, I. W.; Fairclough, J. P. A.; Terrill, N. J.; Ryan, A. J.; Lipic, P. M.; Bates, F. S.; Towns-Andrews, E. *Macromolecules* **1996**, *29*, 8835.
(18) Unger, R.; Beyer, D.; Donth, E. *Polymer* **1991**, *32*, 3305.
(19) Cohen, R. E.; Cheng, P.-L.; Douzinas, K.; Kofinas, P.; Berney, C. V. *Macromolecules* **1990**, *23*, 324.
(20) Veith, C. A.; Cohen, R. E.; Argon, A. S. *Polymer* **1991**, *32*, 1545.
(21) Tsitsilianis, C.; Staikos, G.; Dondos, A.; Lutz, P.; Rempp, P. *Polymer* **1992**, *33*, 3369.
(22) Floudas, G.; Tsitsilianis, C. *Macromolecules* **1997**, *30*, 4381.
(23) Rangarajan, P.; Register, R. A.; Fetters, L. J. *Macromolecules* **1993**, *26*, 4640.
(24) Rangarajan, P.; Register, R. A.; Adamson, D. H.; Fetters, L. J.; Bras, W.; Naylor, S.; Ryan, A. *Macromolecules* **1995**, *28*, 1422.
(25) Rangarajan, P.; Register, R. A.; Fetters, L. J.; Bras, W.; Naylor, S.; Ryan, A. *Macromolecules* **1995**, *28*, 4932.
(26) Quiram, D. J.; Register, R. A.; Marchand, G. R. *Macromolecules* **1997**, *30*, 4551.
(27) Nojima, S.; Kato, K.; Yamamoto, S.; Ashida, T. *Macromolecules* **1992**, *25*, 2237.
(28) Nojima, S.; Nakano, H.; Takahashi, Y.; Ashida, T. *Polymer* **1994**, *35*, 3479.
(29) Liu, L.-Z.; Yeh, F.; Chu, B. *Macromolecules* **1996**, *29*, 5336.
(30) Leibler, L. *Macromolecules* **1980**, *13*, 1602.
(31) Bates, F. S.; Fredrickson, G. H. *Annu. Rev. Chem.* **1990**, *41*, 525.
(32) Chu, B.; Harney, P. J.; Li, Y.; Linliu, K.; Yeh, F.; Hsiao, B. S. *Rev. Sci. Instrum.* **1994**, *65*, 597.
(33) Verma, R.; Marand, H.; Hsiao, B. *Macromolecules* **1996**, *29*, 7767.
(34) Ungar, G.; Keller, A. *Polymer* **1986**, *27*, 1835.
(35) Cheng, S. Z. D.; Zhang, A.; Barley, J. S.; Chen, J.; Habenschuss, A.; Zschack, P. R. *Macromolecules* **1991**, *24*, 3937.
(36) Glatter, O.; Kratky, O. *Small-Angle X-ray Scattering*; Academic Press: London, 1982.
(37) Nojima, S.; Tanaka, H.; Rohadi, A.; Sasaki, S. *Polymer* **1998**, *39*, 1727.

MA980576X